RESEARCH ARTICLE

Check for updates

Air stable and efficient rare earth Eu(II) hydro-tris(pyrazolyl)borate complexes with tunable emission colors†

Hao Qi, [ID] Zifeng Zhao, [ID] Ge Zhan, Boxun Sun, Wenchao Yan, Chengbo Wang, Liding Wang, [ID] Zhiwei Liu, [ID] * Zuqiang Bian [ID] * and Chunhui Huang

Luminescent rare earth Eu(II) complexes with a characteristic 5d−4f transition have shown potential in various applications. However, the exploration and further application of typical Eu(II) complexes are strongly impeded by their instability arising from the easily oxidation of Eu^{2+} ions. In this work, three new Eu(II) complexes bis(hydro-tris(3-phenyl-5-methylpyrazolyl)borate)europium(II) ($Eu(Tp^{Ph,Me})_2$), bis(hydro-tris(3-phenylpyrazolyl)borate)europium(II) ($Eu(Tp^{Ph})_2$), and bis(hydro-tris(3,5-diphenylpyrazolyl)borate)europium(II) ($Eu(Tp^{Ph2})_2$) were designed and synthesized. Their crystal structures, photophysical properties and air stabilities were characterized and discussed. It is found that the introduction of the bulky phenyl group not only increases the air stability by sterically hindering the central Eu^{2+} ions, but also tunes the maximum emission wavelength by influencing the ligand field. This work provides rules for regulating the luminescence properties of Eu(II) complexes as well as design basis for achieving stable and efficient Eu(II) complexes.

Introduction

Rare earth elements are widely used in many luminescent materials due to their abundant orbital energy levels and excellent luminescence characteristics.[1,2] From the perspective of the luminescence mechanism, rare earth elements can be mainly divided into f–f transition and d–f transition ones. For traditional f–f transition rare earth compounds, the f orbitals are in the inner shell and shielded by the filled $5s^2 5p^6$ electron orbitals. This gives rise to special photophysical properties: relatively fixed absorption and emission wavelengths, narrow-line emission, long excited state lifetime and not easily quenched luminescence by concentration or temperature.[1] Based on these characteristics, f–f transition rare earth compounds are widely used in organic electroluminescence,[3,4] biological imaging[5–7] and silicon multicrystalline solar cells.[8]

Different from the f–f transition, the parity-allowed d–f transition gives rare earth compounds a relatively short excited life-time and broadband emission. Since the 5d electron is not protected by the shielding effect, its energy levels can easily be varied with the external environment. Thus, the emission color of d–f transition rare earth compounds can be tuned in a very broad range.[9] These unique properties make d–f transition compounds a good prospect in many fields such as near-infrared-emitting phosphors,[10] visible-light-promoted photoredox catalysis,[11] phosphor-converted white light-emitting diodes (pc-WLEDs)[12] and organic electroluminescence.[13] Despite the great progress, d–f transition rare earth complexes, most of them are divalent rare earth complexes, still have a long way to go. The high instability of these complexes to oxygen is a great challenge for the application of such materials.[14] Among them, the Eu(II) ion has an accessible d–f transition state because of its half-filled $4f^7$ electronic configuration and a considerably higher stabilization from exchange energy with a standard electrode potential of −0.35 V.[15] Currently, the research on Eu(II) complexes mainly focuses on macrocyclic complexes,[16,17] cyclopentadienyl complexes,[18] *etc.* However, the complexes can remain stable in air for a long time are very rare. Solving the stability problem of Eu(II) complexes is the first step to solve the stability problem of divalent rare earth complexes.

Large steric hindrance is an effective way to solve the instability of Eu(II) complexes by protecting the Eu(II) core to minimize its interaction with the environment.[19] Among the reported Eu(II) complexes, Eu(II)-hydro-tris(pyrazolyl)borates

Beijing National Laboratory for Molecular Sciences (BNLMS), State Key Laboratory of Rare Earth Materials Chemistry and Applications, Beijing Engineering Technology Research Centre of Active Display, College of Chemistry and Molecular Engineering, Peking University, Beijing, 100871, China. E-mail: zwliu@pku.edu.cn, bianzq@pku.edu.cn

†Electronic supplementary information (ESI) available. CCDC 2010437–2010439. For ESI and crystallographic data in CIF or other electronic format see DOI: 10.1039/d0qi00762e

This journal is © the Partner Organisations 2020

Inorg. Chem. Front., 2020, **7**, 4593–4599 | 4593

have demonstrated the highest photoluminescence quantum yield (PLQY).[13,20,21] Hence, we chose hydro-tris(pyrazolyl) borates as the skeleton ligand, and introduced the big phenyl group at the 3-position and systematically adjusted the substituent at the 5-position of pyrazole. By investigating the structure, photoluminescence properties, and air stability of the resulting three complexes, it is found that they all showed good stability in air with typical and tunable d–f transitions.
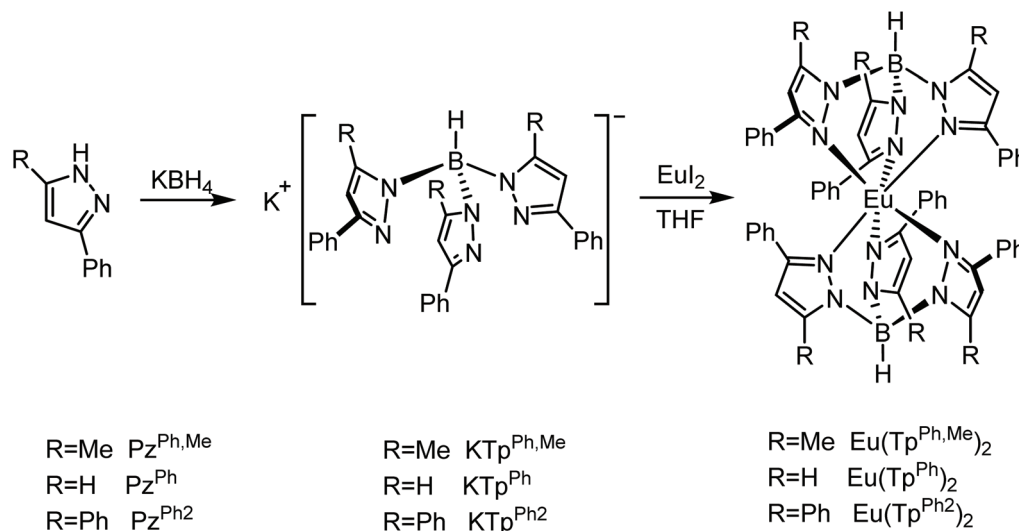
Results and discussion

Synthesis and structures

The three Eu(II) complexes $Eu(Tp^{Ph,Me})_2$, $Eu(Tp^{Ph})_2$ and $Eu(Tp^{Ph2})_2$ were synthesized according to the routes shown in Scheme 1. Single crystals of $Eu(Tp^{Ph,Me})_2$, $Eu(Tp^{Ph})_2$, and $Eu(Tp^{Ph2})_2$ were obtained by the slow evaporation of dichloromethane/hexane solution, toluene solution, and sublimation, and characterized by X-ray diffraction analysis (SC-XRD, Table S1†), respectively. The crystal structures of these three complexes are shown in Fig. 1. As shown in the figure, the complexes are all hexa-coordinated, with six nitrogen atoms belonging to pyrazole. $Eu(Tp^{Ph})_2$ is similar in structure to the reported complexes of $Sm(Tp^{Ph})_2$ and $Yb(Tp^{Ph})_2$, which have the same ligands.[22] From $Eu(Tp^{Ph,Me})_2$, $Eu(Tp^{Ph})_2$ to $Eu(Tp^{Ph2})_2$, the average Eu–N bonds increase gradually from 2.652 Å, 2.662 Å to 2.714 Å, respectively (Table 1, the small difference between $Eu(Tp^{Ph,Me})_2$ and $Eu(Tp^{Ph})_2$ is the result of averaging the difference in bond lengths, as the maximum difference is ∼0.03 Å). Besides, there are six phenyl groups around the Eu^{2+} core protecting it from the environment. With the change of substituents, the molecular structure symmetry of the three complexes increases from $Eu(Tp^{Ph,Me})_2$ to $Eu(Tp^{Ph})_2$ and $Eu(Tp^{Ph2})_2$. Compared with $Eu(Tp^{Ph})_2$, $Eu(Tp^{Ph2})_2$ has a higher symmetry of C_3, while the "bent sandwich-like" structure of $Eu(Tp^{Ph,Me})_2$ decreases its symmetry. Moreover,
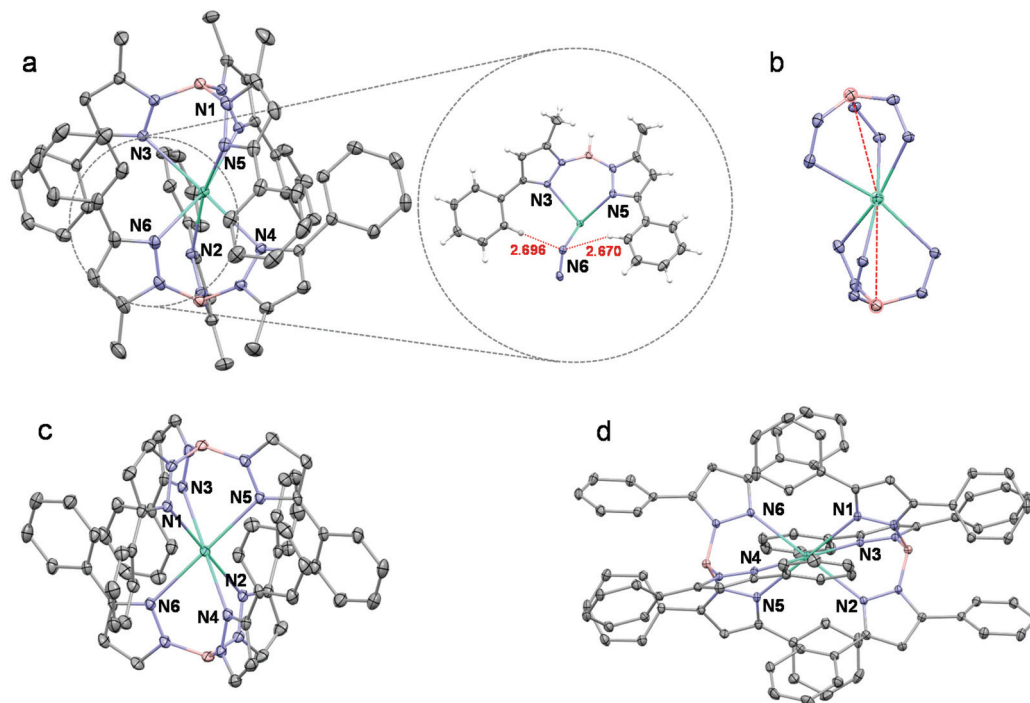
the interligand C–H⋯N bonds (2.696 Å and 2.671 Å, shown in Fig. 1) between the H on the phenyl and the N on the pyrazolyl become another driving force for forming the bent structure.[23,24] The "bent sandwich-like" structure is not usual,[22,25,26] but the same as the divalent Eu, Yb, Sm, and Tm complexes of $Ln(Tp^{iPr2})_2$.[23,27] The B–Eu–B angle of $Eu(Tp^{Ph,Me})_2$ is 164.28°, greater than 151.07° and 153.88° of $Eu(Tp^{iPr2})_2$ in the two independent molecules.[27] A probable reason is that methyl is less sterically hindered than isopropyl. Without the steric effect of the 5-methyl group, $Eu(Tp^{Ph})_2$ adopts a trigonal antiprismatic molecular structure comprising a linear B–Eu–B arrangement. The phenyl groups around the Eu^{2+} core have C_2 symmetry. For $Eu(Tp^{Ph2})_2$, the three 5-phenyl groups at each vertex form a C_3 symmetry axis in an outward-sloping configuration (the face angles between each of the two phenyl groups are all 62.92°), which greatly reduces the repulsion. So $Eu(Tp^{Ph2})_2$ does not adopt a "bent sandwich-like" configuration like $Eu(Tp^{Ph,Me})_2$, but uses a linear configuration. The 3-phenyl groups around the Eu(II) core adopt a C_6 symmetry.

Photophysical properties

It is found that $Eu(Tp^{Ph2})_2$ is almost insoluble in common solvents such as dimethyl sulfoxide, dichloromethane, and toluene, while $Eu(Tp^{Ph,Me})_2$ and $Eu(Tp^{Ph})_2$ showed very weak emissions when dissolved in these solvents; hence the photoluminescence properties of the three complexes were only studied in crystalline powder. The maximum emission peaks (λ_{em}) of $Eu(Tp^{Ph,Me})_2$, $Eu(Tp^{Ph})_2$ and $Eu(Tp^{Ph2})_2$ are located at 617 nm, 578 nm and 538 nm (Table 2 and Fig. 2a), demonstrating emission colors as orange-red, orange, and green (Fig. 2b), respectively. As the emission energy distribution of an Eu(II) complex is generally related to the average bond lengths,[28] this blue shift can be explained in the view of comparing the Eu–N bond lengths in these complexes. Among the

R=Me $Pz^{Ph,Me}$
R=H Pz^{Ph}
R=Ph Pz^{Ph2}

R=Me $KTp^{Ph,Me}$
R=H KTp^{Ph}
R=Ph KTp^{Ph2}

R=Me $Eu(Tp^{Ph,Me})_2$
R=H $Eu(Tp^{Ph})_2$
R=Ph $Eu(Tp^{Ph2})_2$

Scheme 1 Synthetic routes of $Eu(Tp^{Ph,Me})_2$, $Eu(Tp^{Ph})_2$ and $Eu(Tp^{Ph2})_2$.

4594 | *Inorg. Chem. Front.*, 2020, **7**, 4593–4599

This journal is © the Partner Organisations 2020

Fig. 1 Molecular structures of Eu(Tp^{Ph,Me})$_2$ (a, left), Eu(Tp^{Ph})$_2$ (c) and Eu(Tp^{Ph2})$_2$ (d). The illustration of interligand C−H···N bonds (a, right) and the description of the "bent sandwich-like" structure of Eu(Tp^{Ph,Me})$_2$ (b). The atoms are drawn with 30% probability ellipsoids. H atoms are omitted for clarity. The blue-green sphere represents Eu, the pink one represents B, the purple blue one represents N and the gray one represents C.

Table 1 The Eu−N bond distances (Å) in Eu(Tp^{Ph,Me})$_2$, Eu(Tp^{Ph})$_2$ and Eu(Tp^{Ph2})$_2$

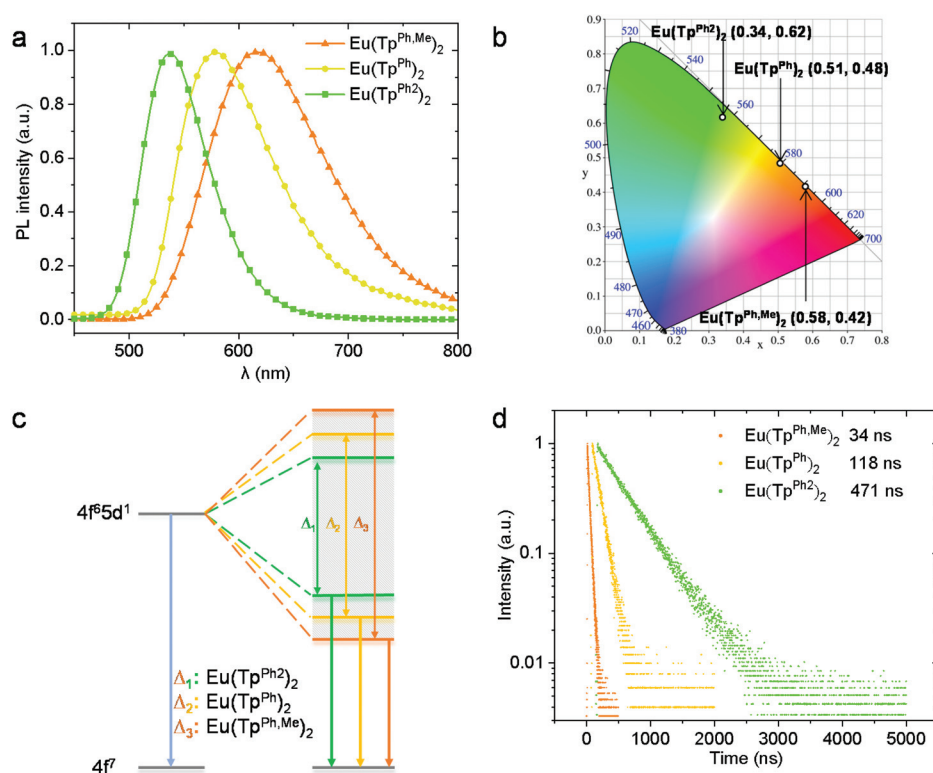|	Eu(Tp^{Ph,Me})$_2$	Eu(Tp^{Ph})$_2$	Eu(Tp^{Ph2})$_2$
Eu–N1	2.632	2.634	2.712
Eu–N2	2.632	2.634	2.712
Eu–N3	2.655	2.657	2.713
Eu–N4	2.655	2.657	2.714
Eu–N5	2.666	2.695	2.715
Eu–N6	2.666	2.695	2.715
Eu–N (average)	2.652	2.662	2.714

three complexes, the average Eu–N bond lengths for Eu(Tp^{Ph,Me})$_2$, Eu(Tp^{Ph})$_2$ and Eu(Tp^{Ph2})$_2$ increased gradually. Since a shorter bond length makes a stronger ligand field splitting of the d orbitals, the energy levels of the lowest energy 5d orbital increase in the order of Eu(Tp^{Ph,Me})$_2$, Eu(Tp^{Ph})$_2$ and Eu(Tp^{Ph2})$_2$ (Fig. 2c). So, the transition energy from the lowest energy d orbitals to f orbitals increases, assuming that the energy of f orbitals is unchanged in these complexes, which results in the observed blue shift in emission spectra. In addition, all the three complexes showed broadband emissions, with the full widths at half maximum (FWHMs) gradually decreasing from Eu(Tp^{Ph,Me})$_2$ (125 nm) to Eu(Tp^{Ph})$_2$ (101 nm) and Eu(Tp^{Ph2})$_2$ (70 nm). Such a broad emission band is typical of the 5d–4f transition of the Eu(II) core, and the tendency from Eu(Tp^{Ph,Me})$_2$ to Eu(Tp^{Ph2})$_2$ might be caused by the increasing rigidity in turn. By comparing the excitation spectra of the three Eu(II) complexes and their corresponding ligands (Fig. S1†), an obvious broadening of the spectra was observed, indicating that both excitation from the ligand and the central Eu^{2+} ion are accessible to achieve an efficient 5d–4f transition in the three Eu(II) complexes.

The excited state lifetimes (τ) of these three complexes were also measured (Fig. 2d and Table 2). Coincidentally, an increased lifetime from Eu(Tp^{Ph,Me})$_2$ (34 ns) to Eu(Tp^{Ph})$_2$ (118 ns) and Eu(Tp^{Ph2})$_2$ (471 ns) was observed. These lifetimes are comparable to those of the reported Eu(II) complexes,[16] but the huge differences in these three complexes are worthy of further study. Therefore, PLQYs were measured to deduce the

Table 2 Photophysical data of Eu(Tp^{Ph,Me})$_2$, Eu(Tp^{Ph})$_2$ and Eu(Tp^{Ph2})$_2$ in crystalline powder

Complex	λ_{ex} (nm)	λ_{em} (nm)	τ (ns)	PLQY (%)	FWHMs (nm)	k_r (10^6 s^{-1})	k_{nr} (10^6 s^{-1})
Eu(Tp^{Ph,Me})$_2$	465	617	34	3	125	0.88	28.5
Eu(Tp^{Ph})$_2$	440	578	118	20	101	1.69	6.78
Eu(Tp^{Ph2})$_2$	414	538	471	70	70	1.49	0.63

This journal is © the Partner Organisations 2020

Inorg. Chem. Front., 2020, **7**, 4593–4599 | **4595**

Fig. 2 (a) Solid steady-state PL spectra (photoexcitation wavelength: 365 nm) of Eu(Tp^{Ph,Me})$_2$, Eu(Tp^{Ph})$_2$ and Eu(Tp^{Ph2})$_2$. (b) The CIE 1931 chromaticity diagram of Eu(Tp^{Ph,Me})$_2$, Eu(Tp^{Ph})$_2$ and Eu(Tp^{Ph2})$_2$. (c) Orbital-energy diagram for the ligand field splitting of the d orbitals (double arrow) and the energy transition (single arrow) of Eu(Tp^{Ph,Me})$_2$, Eu(Tp^{Ph})$_2$ and Eu(Tp^{Ph2})$_2$. (d) Transient PL spectra of Eu(Tp^{Ph,Me})$_2$, Eu(Tp^{Ph})$_2$ and Eu(Tp^{Ph2})$_2$.

radiative rate constant (k_r) and non-radiative rate constant (k_{nr}). Among these complexes, Eu(Tp^{Ph2})$_2$ showed a high PLQY of 70%, which is the highest value for an green emission Eu(II) complex up to now, while Eu(Tp^{Ph,Me})$_2$ and Eu(Tp^{Ph})$_2$ showed a relatively lower PLQY of 3% and 20%, respectively. So far, the maximum PLQY of Eu(II) complexes is 96%,[21] but the PLQYs of most Eu(II) complexes are relatively low, below 50% (Table S2†). The radiative rate constants, calculated from the aforementioned data, are shown in Table 2. In order to better understand the regularities, we also introduced a published complex bis(hydro-tris(3,5-dimethylpyrazolyl)borate)europium(II) (Eu(Tp^{Me2})$_2$) with good photoluminescence properties for comparison[13] (τ = 987 ns, PLQY = 85%, k_r = 0.86 × 10^6 s^{-1}, k_{nr} = 0.15 × 10^6 s^{-1}). It can be concluded that their radiative rate constants are similar, while the non-radiative rate constants vary in an order of magnitude. We propose that increased rigidity decreases the non-radiative transition rate. 5-Phenyl in Eu(Tp^{Ph2})$_2$ and 5-methyl in Eu(Tp^{Ph,Me})$_2$ would increase the molecular rigidity. But the forming "bent sandwich-like" structure can be more randomly arranged in space, which allows us to ignore the rigidity of the methyl group. So the rigidity increases from Eu(Tp^{Ph,Me})$_2$, Eu(Tp^{Ph})$_2$ to Eu(Tp^{Ph2})$_2$. As for Eu(Tp^{Me2})$_2$, the decreased non-radiative transition rate may be due to a stronger combination between Eu(II) and the coordination N atoms in the ligands (the average length of Eu–N

bonds is 2.585 Å, much shorter than those for Eu(Tp^{Ph,Me})$_2$, Eu(Tp^{Ph})$_2$ and Eu(Tp^{Ph2})$_2$).[16]

Air stability and its rationalization

It is well known that the air stability of typical Eu(II) complexes is poor because the standard electrode potential of Eu^{2+} is as low as −0.35 V. So we introduced phenyl as a large steric hindrance group around Eu(II) to improve its air stability. In view of this, the complex Eu(Tp^{Me2})$_2$ was adopted as a reference. The luminescence stability of the complexes was described by the change of the PLQY in air and which is further used to understand the stability of the complexes. As shown in Fig. 3a, the PLQY of Eu(Tp^{Me2})$_2$ decreased to 7% of its original value after one day and to only 3% after 4 days. In contrast, the PLQY of Eu(Tp^{Ph2})$_2$ decreased to 94% after one day and to 87% even after 10 days. After the tenth day of measurement, Eu(Tp^{Ph2})$_2$ was placed in a glove box and taken out the next day to measure its PLQY. To our delight, the PLQY returned to the original value. This indicates that the decrease of the PLQY of Eu(Tp^{Ph2})$_2$ is not caused by the oxidation of Eu(II) but probably due to the quenching effect of oxygen or water in air. To investigate further, two atmospheres, one with pure oxygen and another with water-containing nitrogen, were created. Then Eu(Tp^{Ph2})$_2$ was loaded into the two atmospheres for 3 hours. It was found that the PLQYs of the samples in a pure oxygen
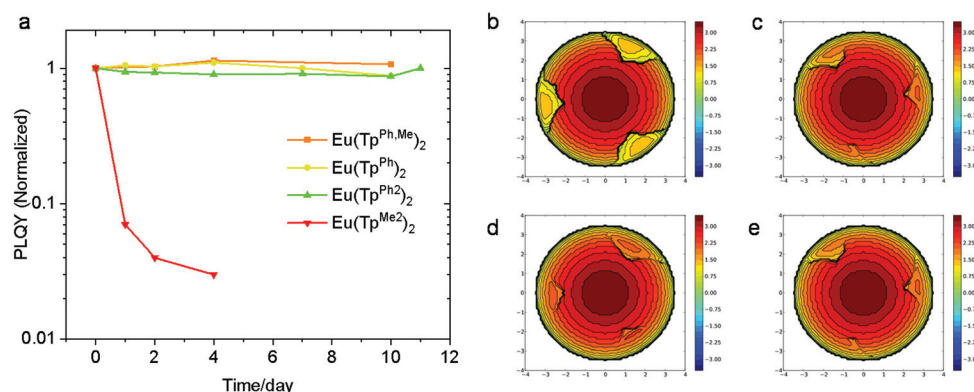
Fig. 3 (a) The normalized PLQY changes of crystalline $Eu(Tp^{Me2})_2$, $Eu(Tp^{Ph,Me})_2$, $Eu(Tp^{Ph})_2$ and $Eu(Tp^{Ph2})_2$ in air. Topographic steric maps of $Eu(Tp^{Me2})_2$ (b), $Eu(Tp^{Ph,Me})_2$ (c), $Eu(Tp^{Ph})_2$ (d) and $Eu(Tp^{Ph2})_2$ (e). Red and blue indicate the more- and less-hindered zones, respectively.[29]

atmosphere and water-containing nitrogen atmosphere were reduced to 52% and 85% of the initial value, respectively. After the test, the samples were transferred into a glove box (under a nitrogen atmosphere and at room temperature, with the oxygen concentration below 1.0 ppm and the water concentration below 0.1 ppm), and their PLQYs were measured again a day later. The PLQYs of both the samples returned to the initial values. Based on this phenomenon, we propose that the complex can absorb oxygen and water and both oxygen and water can quench the luminescence of the complex to a certain extent, in which oxygen is the main quencher. When the sample is returned to the glove box, oxygen and water are desorbed from the surface of the complex, allowing the PLQY of $Eu(Tp^{Ph2})_2$ to recover. The PLQYs of $Eu(Tp^{Ph,Me})_2$ and $Eu(Tp^{Ph})_2$ were kept almost the same to the original data (the accurate PLQY values of the four complexes are shown in Table S3†). To further understand the air stability of these complexes, time dependent XRD spectra were obtained as shown in Fig. S2.† During the four-day test, the XRD peak position did not change, and no new peak was observed. In addition, mass change monitoring upon isothermal exposion of the complexes under an air flow has also been conducted (Fig. S3†). The maximum weight change is 0.0060 mg, which is within the allowable range of measurement error of the instrument. These findings further demonstrate the good air stability of the three complexes.

In order to understand the excellent air stability of the three complexes, we investigated the extent to which the central metal is coated in the three complexes and $Eu(Tp^{Me2})_2$. The spacefill views along the largest exposed area of the four complexes are shown in Fig. S4.† At a glance, the exposed area of $Eu(Tp^{Me2})_2$ is much larger than those of the other three complexes. To further understand the protection of the ligands to the central Eu^{2+} ions, buried volume descriptor (% V_{Bur}) was introduced to quantify the steric hindrance.[30] With the help of SambVca 2.1,[31] the topographic steric maps of the four complexes are drawn in Fig. 3b–e, and the calculated % V_{Bur} values of $Eu(Tp^{Me2})_2$, $Eu(Tp^{Ph,Me})_2$, $Eu(Tp^{Ph})_2$ and $Eu(Tp^{Ph2})_2$ are 84.1%, 91.0%, 91.7% and 92.9%, respectively.[30]

Based on these results, it can be seen that the contribution of the methyl and phenyl groups to steric hindrance is very different. By substituting the methyl group with the phenyl group at the 3-position of pyrazole, $Eu(Tp^{Ph,Me})_2$ showed an obviously increased % V_{Bur} as compared with $Eu(Tp^{Me2})_2$. However, the further substitution of the methyl group with the phenyl group at the 5-position shows only a little difference in % V_{Bur}. Thus, the steric hindrance is mainly caused by introducing the phenyl group at the 3-position of pyrazole.[29]

Conclusions

In summary, three new $Eu(II)$ complexes $Eu(Tp^{Ph,Me})_2$, $Eu(Tp^{Ph})_2$, and $Eu(Tp^{Ph2})_2$ were designed and successfully synthesized. Due to different steric hindrances of the ligand, these complexes adopt a "bent sandwich-like" structure for $Eu(Tp^{Ph,Me})_2$, and a linear configuration for $Eu(Tp^{Ph})_2$ and $Eu(Tp^{Ph2})_2$. All the complexes exhibited broad peak emission with the excited state lifetime in dozens to hundreds of nanoseconds, which is a typical 5d–4f transition characteristic. From $Eu(Tp^{Ph,Me})_2$, $Eu(Tp^{Ph})_2$, to $Eu(Tp^{Ph2})_2$, the average Eu–N length increases gradually, leading to decreased splitting energy of the d orbital, hence a blue shifted emission spectrum. However, the rigidity increases gradually in the order of $Eu(Tp^{Ph,Me})_2$, $Eu(Tp^{Ph})_2$, and $Eu(Tp^{Ph2})_2$, resulting in a significant increase in the excited state lifetime and PLQY. Consequently, $Eu(Tp^{Ph2})_2$ showed the highest PLQY up to 70%. To our delight, all the three complexes showed excellent stability in air, as demonstrated by measuring their time dependent PLQYs, XRD spectra and mass change in the presence of air. By comparing the spacefill views and buried volume descriptors of the three complexes with a reference $Eu(II)$ complex $Eu(Tp^{Me2})_2$, it is found that the introduction of a phenyl group at the 3-position of pyrazole accounts for the improved stability. This work systematically reports the relationships between the photoluminescence/air stability and the structure of molecular $Eu(II)$ complexes, which gives the feasibility to discover

This journal is © the Partner Organisations 2020

Inorg. Chem. Front., 2020, **7**, 4593–4599 | **4597**

highly efficient and air stable luminescent Eu(II) complexes with specific emission colors.

Conflicts of interest

There are no conflicts to declare.

Acknowledgements

References

1 J. C. G. Bunzli and C. Piguet, Taking advantage of luminescent lanthanide ions, *Chem. Soc. Rev.*, 2005, **34**, 1048–1077.

2 Y. Ding, N. Guo, M. Zhu, W. Lv, R. Ouyang, Y. Miao and B. Shao, Luminescence and temperature sensing abilities of zincate phosphors co-doped bismuth Bi^{3+} and lanthanide Eu^{3+}/Sm^{3+}, *Mater. Res. Bull.*, 2020, **129**, 110869.

3 H. Wei, G. Yu, Z. Zhao, Z. Liu, Z. Bian and C. Huang, Constructing lanthanide Nd(III), Er(III) and Yb(III) complexes using a tridentate N, N, O-ligand for near-infrared organic light-emitting diodes, *Dalton Trans.*, 2013, **42**, 8951–8960.

4 L. Wang, Z. Zhao, C. Wei, H. Wei, Z. Liu, Z. Bian and C. Huang, Review on the electroluminescence study of lanthanide complexes, *Adv. Opt. Mater.*, 2019, **7**, 1801256.

5 J. Yu, D. Parker, R. Pal, R. A. Poole and M. J. Cann, A europium complex that selectively stains nucleoli of cells, *J. Am. Chem. Soc.*, 2006, **128**, 2294–2299.

6 A. Picot, A. D'Aléo, P. L. Baldeck, A. Grichine, A. Duperray, C. Andraud and O. Maury, Long-lived two-photon excited luminescence of water-soluble europium complex: applications in biological imaging using two-photon scanning microscopy, *J. Am. Chem. Soc.*, 2008, **130**, 1532–1533.

7 N. Hamon, A. Roux, M. Beyler, J.-C. Mulatier, C. Andraud, C. Nguyen, M. Maynadier, N. Bettache, A. Duperray, A. Grichine, S. Brasselet, M. Gary-Bobo, O. Maury and R. Tripier, Pyclen-based Ln(III) complexes as highly luminescent bioprobes for in vitro and in vivo one- and two-photon bioimaging applications, *J. Am. Chem. Soc.*, 2020, **142**, 10184–10197.

8 G. Katsagounos, E. Stathatos, N. B. Arabatzis, A. D. Keramidas and P. Lianos, Enhanced photon harvesting in silicon multicrystalline solar cells by new lanthanide complexes as light concentrators, *J. Lumin.*, 2011, **131**, 1776–1781.

9 L. Wang, R. J. Xie, T. Suehiro, T. Takeda and N. Hirosaki, Down-conversion nitride materials for solid state lighting: recent advances and perspectives, *Chem. Rev.*, 2018, **118**, 1951–2009.

10 J. W. Qiao, G. J. Zhou, Y. Y. Zhou, Q. Y. Zhang and Z. G. Xia, Divalent europium-doped near-infrared-emitting phosphor for light-emitting diodes, *Nat. Commun.*, 2019, **10**, 5267.

11 T. C. Jenks, M. D. Bailey, J. L. Hovey, S. Fernando, G. Basnayake, M. E. Cross, W. Li and M. J. Allen, First use of a divalent lanthanide for visible-light-promoted photoredox catalysis, *Chem. Sci.*, 2018, **9**, 1273–1278.

12 G. Li, Y. Tian, Y. Zhao and J. Lin, Recent progress in luminescence tuning of Ce^{3+} and Eu^{2+}-activated phosphors for pc-WLEDs, *Chem. Soc. Rev.*, 2015, **44**, 8688–8713.

13 C. P. Shipley, S. Capecchi, O. V. Salata, M. Etchells, P. J. Dobson and V. Christou, Orange electroluminescence from a divalent europium complex, *Adv. Mater.*, 1999, **11**, 533–536.

14 L. A. Basal and M. J. Allen, Synthesis, characterization, and handling of Eu^{II}-containing complexes for molecular imaging applications, *Front. Chem.*, 2018, **6**, 65.

15 J. Garcia and M. J. Allen, Developments in the coordination chemistry of europium(II), *Eur. J. Inorg. Chem.*, 2012, **2012**, 4550–4563.

16 J. Jiang, N. Higashiyama, K. Machida and G. Adachi, The luminescent properties of divalent europium complexes of crown ethers andcryptands, *Coord. Chem. Rev.*, 1998, **170**, 1–29.

17 L. A. Ekanger, L. A. Polin, Y. Shen, E. M. Haacke, P. D. Martin and M. J. Allen, A Eu^{II}-containing cryptate as a redox sensor in magnetic resonance imaging of living tissue, *Angew. Chem., Int. Ed.*, 2015, **54**, 14398–14401.

18 R. P. Kelly, T. D. M. Bell, R. P. Cox, D. P. Daniels, G. B. Deacon, F. Jaroschik, P. C. Junk, X. F. Le Goff, G. Lemercier, A. Martinez, J. Wang and D. Werner, Divalent tetra- and penta-phenylcyclopentadienyl europium and samarium sandwich and half-sandwich complexes: synthesis, characterization, and remarkable luminescence properties, *Organometallics*, 2015, **34**, 5624–5636.

19 N.-D. H. Gamage, Y. Mei, J. Garcia and M. J. Allen, Oxidatively Stable, Aqueous europium(II) complexes through steric and electronic manipulation of cryptand coordination chemistry, *Angew. Chem., Int. Ed.*, 2010, **49**, 8923–8925.

20 M. Suta, M. Kuhling, P. Liebing, F. T. Edelmann and C. Wickleder, Photoluminescence properties of the "bent sandwich-like" compounds $[Eu(Tp^{iPr2})_2]$ and $[Yb(Tp^{iPr2})_2]$ - Intermediates between nitride-based phosphors and metallocenes, *J. Lumin.*, 2017, **187**, 62–68.

21 G. Zhan, L. Wang, Z. Zhao, P. Fang, Z. Bian and Z. Liu, Highly Efficient and Air-Stable Lanthanide Eu^{II} Complex: New Emitter in Organic Light Emitting Diodes, *Angew. Chem.*, 2020, **59**, 1–6.

22 A. C. Hillier, X. W. Zhang, G. H. Maunder, S. Y. Liu, T. A. Eberspacher, M. V. Metz, R. McDonald, A. Domingos, N. Marques, V. W. Day, A. Sella and J. Takats, Synthesis and structural comparison of a series of divalent $Ln(Tp^{R,R'})_2$ (Ln = Sm, Eu, Yb) and trivalent $Sm(Tp^{Me2})_2X$ (X = F, Cl, I, BPh_4) complexes, *Inorg. Chem.*, 2001, **40**, 5106–5116.

23 A. Momin, L. Carter, Y. Yang, R. McDonald, S. Essafi, F. Nief, I. Del Rosal, A. Sella, L. Maron and J. Takats, To bend or not to bend: experimental and computational studies of structural preference in Ln(Tp^{iPr2})$_2$ (Ln = Sm, Tm), *Inorg. Chem.*, 2014, **53**, 12066–12075.

24 R. Taylor and O. Kennard, Crystallographic evidence for the existence of C-H···O, C-H···N, and C-H···Cl hydrogen-bonds, *J. Am. Chem. Soc.*, 1982, **104**, 5063–5070.

25 J. Takats, X. W. Zhang, V. W. Day and T. A. Eberspacher, Synthesis and structure of bis[hydrotris(3,5-dimethyl-pyrazolyl)borato]samarium(II), Sm[HB(3,5-Me$_2$pz)$_3$]$_2$, and the product of its reaction with azobenzene, *Organometallics*, 1993, **12**, 4286–4288.

26 G. H. Maunder, A. Sella and D. A. Tocher, Synthesis and molecular-structures of a redox-related pair of lanthanide complexes, *J. Chem. Soc., Chem. Commun.*, 1994, 885–886.

27 M. Kuhling, C. Wickleder, M. J. Ferguson, C. G. Hrib, R. McDonald, M. Suta, L. Hilfert, J. Takats and F. T. Edelmann, Investigation of the "bent sandwich-like" divalent lanthanide hydro-tris(pyrazolyl)borates Ln(Tp^{iPr2})$_2$ (Ln = Sm, Eu, Tm, Yb), *New J. Chem.*, 2015, **39**, 7617–7625.

28 K. A. Denault, J. Brgoch, M. W. Gaultois, A. Mikhailovsky, R. Petry, H. Winkler, S. P. DenBaars and R. Seshadri, Consequences of optimal bond valence on structural rigidity and improved luminescence properties in Sr$_x$Ba$_{2-x}$SiO$_4$: Eu^{2+} orthosilicate phosphors, *Chem. Mater.*, 2014, **26**, 2275–2282.

29 A. Poater, F. Ragone, R. Mariz, R. Dorta and L. Cavallo, Comparing the enantioselective power of steric and electrostatic effects in transition-metal-catalyzed asymmetric synthesis, *Chem. – Eur. J.*, 2010, **16**, 14348–14353.

30 A. Poater, F. Ragone, S. Giudice, C. Costabile, R. Dorta, S. P. Nolan and L. Cavallo, Thermodynamics of N-heterocyclic carbene dimerization: the balance of sterics and electronics, *Organometallics*, 2008, **27**, 2679–2681.

31 A. Poater, B. Cosenza, A. Correa, S. Giudice, F. Ragone, V. Scarano and L. Cavallo, SambVca: A Web Application for the calculation of the buried volume of N-heterocyclic carbene ligands, *Eur. J. Inorg. Chem.*, 2009, **2009**, 1759–1766.

This journal is © the Partner Organisations 2020

Inorg. Chem. Front., 2020, **7**, 4593–4599 | **4599**